Clinics in Oncology

Research Article
Published: 07 Feb, 2022

PEGylation of AS16 Double-Target Peptide that Blocks the Neuropilin-1 and Tie2 Signaling Pathways Enhances its Antitumor Effect

Guodong Li, Shuyi Song, Baomei Yuan, Guangming Wan and Shenghua Zhang*

School of Life Sciences, Zhengzhou University, China

Abstract

Immunotherapy has become a major treatment in oncology. However, most cancer patients do not currently benefit from this treatment. In most patients with solid tumors, abnormal blood vessels help the tumor evade the attack of the immune system, with the blood vessel abnormalities being the result of elevated angiogenic factors such as Vascular Endothelial Growth Factor (VEGF) and angiopoietin 2. The use of drugs targeting these molecules normalizes the abnormal tumor vascular system to increase the infiltration of immune effect or cells and improve the responsiveness of immunotherapy. AS16 is a double-target peptide that is able to block both the VEGF and Tie2 signaling pathways, demonstrating significant anti-angiogenesis and antitumor effects. However, owing to its poor stability and short half-life, its clinical application is limited. To solve these problems, we used fixed-point modification of AS16 with Polyethylene Glycol (PEG) of different molecular weights to obtain PEG-AS16. The stability and half-life of the obtained PEG-AS16 were both longer than those of AS16. In addition, the biological activity of PEG-AS16 and its anti-angiogenesis and anti tumor effects were demonstrated by wound healing assay of alginate-coated tumor cells. Our results suggest that PEG-AS16 has potential as an effective anti-angiogenesis drug.

Keywords: Anti-angiogenesis; PEGylation; Anti-tumor; Peptide

Introduction

Many patients with solid tumors have failed to respond to checkpoint inhibitors, although their efficacy and potential for assisting the human immune system in anticancer therapy have been demonstrated. One reason for this is that tumors develop abnormal vasculature, where abnormal blood vessels and impaired perfusion restrict the flow of cytotoxic drugs and immune cells from the bloodstream into the tumor, limiting their anticancer activity [1]. Anti-angiogenesis can normalize the blood vessel network around a tumor and improve the tumor microenvironment and the infiltration and activity of type 1 T helper lymphocytes to improve the efficacy of checkpoint inhibitors and the response rate of treatment [2].

Peptide A7R (ATWLPPR) can specifically bind to Neuropilin-1 (NRP1) and block its interaction with Vascular Endothelial Growth Factor 165 (VEGF165), thus demonstrating significant anti-angiogenesis and antitumor activity [3]. Meanwhile, peptide NS7 (NLLMAAS) can specifically block the Tie2 signaling pathway, inhibiting the migration of endothelial cells and the formation of blood vessels, as has been shown in chicken embryo allantoic membrane [4]. In the early stages of our study, we linked peptide A7R and peptide NS7 with two alanine to obtain a new peptide AS16 (ATWLPPRAANLLMAAS) that can inhibit both the VEGF/NRP1 and Angiopoeitin-2 (Ang2)/Tie2 signaling pathways. Previous studies have shown that AS16 can also inhibit endothelial cell migration and tubular formation and significantly inhibit tumor growth. Compared with peptide A7R and NS7, it has been demonstrated that AS16 has stronger anti-angiogenesis and antitumor activity effects [5]. However, like other peptide drugs, AS16 also has many issues. For example, it is prone to degradation by protease, is easily filtered by glomeruli, and has poor stability, low molecular weight, and a short half-life. As a result, peptide drugs cannot make full use of their potential efficacy *in vivo*, which means that effective and feasible modifications of the drugs need to be implemented [6].

PEGylation involves protein, peptide, or non-peptide small molecules modified by the covalent attachment of one or more Polyethylene Glycols (PEG). These modification types include

Correspondence:
Guodong Li, School of Life Sciences, Zhengzhou University, 100 Science Road, Zhengzhou 450001, China, E-mail: ligd@zzu.edu.cn

Received Date: *20 Dec 2021*
Accepted Date: *17 Jan 2022*
Published Date: *07 Feb 2022*

Citation:
Li G, Song S, Yuan B, Wan G, Zhang S. PEGylation of AS16 Double-Target Peptide that Blocks the Neuropilin-1 and Tie2 Signaling Pathways Enhances its Antitumor Effect. Clin Oncol. 2022; 7: 1893.

ISSN: 2474-1663

random modification, fixed-point modification, enzymatic PEG modification, and non-covalent PEG modification [7-13]. For example, certolizumab pegol (marketed in 2008) is a fixed-point modification of Fab fragment C-terminal Cyst Mercator that uses a 40 kDa branched PEG-MAL against tumor necrosis factor antibodies [14]. PEG also has a large kinetic volume in aqueous solution and is nontoxic and immunogenic [10,15]. PEG modification can also improve the pharmacokinetic properties of peptides and protein drugs *in vivo*. The shielding effect of PEG on the surface of peptides and proteins reduces enzymatic hydrolysis rate, improves stability, and reduces glomerular filtration rate, thus increasing the half-life of peptides and improving the metabolic characteristics of drugs *in vivo*. So far, more than 10 PEG-modified proteins have been approved by the food and drug administration for clinical use [16-18].

In this study, we applied PEG modification technology to AS16, introducing Cysteine (Cys) at the N-terminal of AS16 by chemical synthesis and fixing the Mercator group of the introduced Cys with different molecular weights using monomethoxy Polyethylene Glycol Maleimide (mPEG-MAL). The stability, metabolism, biological activity, and *in vivo* antitumor effect of the modified compound were tested, and a polyethylene glycol modification, mPEG-AS16, with a longer half-life, better antitumor angiogenesis, and tumor inhibition effect was obtained.

Materials and Methods

Reagents and cell culture

AS16 and Cys-AS16 were purchased from Shanghai Ketai Biotechnology Co., Ltd., and mPEG-MAL (5 and $_{20k}$Da) was purchased from Tianjin Hongri Jinboda Biotechnology Co., Ltd. Human plasma was isolated from blood supplied by volunteers. Sodium alginate and FITC-dextran were purchased from Sigma-Aldrich, and RPMI-1640 medium was purchased from Solarbio. Penicillin/streptomycin was purchased from Gibico. HUVEC and S180 cells were preserved in our laboratory, and the cells were cultured in RPMI-1640 medium containing 10% FBS and 100 IU penicillin/streptomycin at 37°C in a 5% CO_2 atmosphere.

Effects of molar ratio and reaction temperature on modification reaction

Cys-AS16 was dissolved in PBS (pH 6.0, 20 mM) to a final concentration of 1 mg/mL. Cys-AS16 and mPEG-MAL in molar ratios of 1:1, 1.5:1, and 2:1 were added to the Cys-AS16 solution (1 mL) and left to react for 1h at 25°C. This was then sampled using RP-HPLC (C18 analytical column: 250 mm × 4.6 mm × 5 μm; Zhengzhou Yingnuo Biotechnology Co., Ltd.; Agilent LC 1200 liquid chromatography). 1 mL of the above Cys-AS16 solution was then collected and allowed to react with mPEG-MAL with a Cys-AS16: mPEG-MAL molar ratio of 1:2. The reaction was first carried out at 4°C for 1 h and then at 25°C for 1 h, and the samples were analyzed using RP-HPLC.

Separation and purification of modifications

The modification reaction was carried out in accordance with the optimum reaction conditions that had been determined. After the completion of the reaction, the modified compounds were isolated and purified by preparative RP-HPLC. The purification conditions were as follows: (1) Mobile phase A: 0.1% TFA aqueous solution, (2) mobile phase B: Acetonitrile, (3) wavelength: 228 nm, (4) flow rate: 5 mL/min, (5) column temperature: 25°C, (6) injection volume: 10 mL, and (7) elution gradient: 0~30 min, 20%~60% B. The purified modifications were analyzed for purity using RP-HPLC and then stored using lyophilization.

Enzyme hydrolysis stability test

100 μL of each of AS16, mPEG$_{5k}$-AS16, and mPEG$_{20k}$-AS16 in equimolar concentration (2.4 μmol/L) were added to 900 μL of plasma and rapidly vortexed. The time point at which the peptide was added to the plasma was recorded as 0 h. The peptide plasma mixture was quickly incubated in 37°C, and 100 μL samples were taken at different time points. Next, 50 μL of a 10% perchloric acid solution was added to 100 μL of the mixture, and the mixture was thoroughly vortexed and then centrifuged at 12,000 rpm for 15 min. 100 μL of the supernatant was then aspirated and stored at -80°C. The concentration of AS16 and its analogues in the supernatant was determined by RP-HPLC.

Determination of pharmacokinetic parameters

Sprague Dawley (SD) rats weighing approximately 250 g each were purchased from the Experimental Animal Center of Henan Province. The rats were fasted for 12 h before the experiment and were free to drink water during the experiment. Blood was taken from the orbital venous plexus of the rats. The blood sample was placed in an Eppendorf (EP) tube containing heparin sodium. After mixing, the cells were centrifuged at 6000 rpm for 3 min. The supernatant, blank plasma was stored at -20°Cuntil use. AS16, mPEG$_{5k}$-AS16, and mPEG$_{20k}$-AS16 were dissolved in saline, formulated into equimolar solutions, and then stored at -80°C until use.

The AS16, mPEG$_{5k}$-AS16, and mPEG$_{20k}$-AS16 solutions were diluted with blank plasma to prepare a series of standard concentrations of three parts each. 25 μL of 10% perchloric acid was added to 50 μL of the mixture, vortexed, and then centrifuged at 12,000 rpm for 15 min, after which 20 μL of the supernatant was analyzed using RP-HPLC. A standard curve was prepared based on peak area and concentration (μmol/mL) data.

AS16, mPEG$_{5k}$-AS16, and mPEG$_{20k}$-AS16 solutions (standards of 40 mg/kg AS16; 23.7 μmol/kg) were injected into the SD rats *via* the tail vein. Blood was taken from the orbital venous plexus of the rats before administration (0 h) and at different time points after administration. The blood sample was placed in an EP tube containing heparin sodium, mixed, and centrifuged at 6000 rpm for 3 min. 50 μL of the supernatant was then added to 25 μL of 10% perchloric acid, mixed, and centrifuged at 12,000 rpm for 15 min, and 20 μL of the supernatant was taken and analyzed using RP-HPLC. The chromatographic conditions were as follows: (1) Wavelength: 228 nm, (2) flow rate: 1 mL/min, (3) column temperature: 30°C, (4)injection volume: 20 μL, (5) mobile phase A: 0.1% TFA aqueous solution, (6) mobile phase B: Acetonitrile + 0.1% TFA, (7) elution gradient of AS16: 0~30 min, 20%~60% B, and (8) elution gradients of mPEG$_{5k}$-AS16 and mPEG$_{20k}$-AS16: 0~5 min, 20%~40% B; 5~15 min, 40%~50% B; and 15~20 min, 50%~60% B.

Wound healing assay

HUVEC cells with a positive growth rate were taken, and cell density was adjusted to 1 × 10^5 cells/mL using RPMI-1640 medium after digestion. The cell suspension was added to a 24-well plate (1 mL per well) and allowed to sit for 24 h. After 24 h, cell enrichment was about 95% and was a continuous monolayer. A 200 μL pipette tip was used to "+" the line on the cells. This was then washed twice with PBS and replaced with RPMI-1640 medium without FBS. Different concentrations (5, 25, and 100 μM) of AS16, mPEG$_{5k}$-AS16, and

$mPEG_{20k}$-AS16 were added to the wells, and three replicate wells were set for each concentration. Three measurements of the wound width were randomly selected for each well under the microscope and recorded as W_{0h}. After 24 h, the width of the scratch at the same place of each well was measured and recorded as W_{24h}. Mobility was calculated as follows: mobility (%).

$= [1-W_{24h}/W_{0h}] \times 100\%$.

Alginate-coated tumor cells

Female Balb/c mice aged 6~8 weeks were purchased from Beijing Weitonglihua Biotechnology Co., Ltd. The density of S180 cells was adjusted to 1×10^7 cells/mL, and 0.2 mL of the cell suspension was injected into the abdominal cavities of the mice. One week later, a slight swelling of the mice abdomens was observed. After the ascites was aspirated and diluted with saline at a ratio of 1:5, 0.2 mL of the diluted ascites was injected into the abdominal cavity of Balb/c mice for a second passage. After 5~7 days, the ascites of the mice were taken, diluted with saline, and centrifuged at 1,000 rpm for 5 min, and the supernatant was discarded.

The alginate was dissolved in saline to prepare a 1.5% alginate solution. Then, the precipitated S180 cells were re-suspended in a 1.5% alginate solution to adjust the cell density to 1×10^7 cells/mL. Next, the S180 cell suspension was slowly dropped into 80 mM Calcium Chloride ($CaCl_2$) solution and then stirred. The white alginate particles that had formed were allowed to stand at room temperature for 30 min to solidify.

Balb/c mice were intraperitoneally injected with an appropriate amount of chloral hydrate for anesthesia. The right upper back skin of the mice was sterilized with 75% alcohol, and a small opening was cut. Alginate particles were planted under the skin of mice at three particles per mouse, and the incisions were sterilized. The mice were randomly divided into four groups, with eight mice in each group. These groups were the NS group, the AS16 group (0.3 μmol/kg/d), the $mPEG_{5k}$-AS16 group (0.3 μmol/kg/d), and the $mPEG_{20k}$-AS16 group (0.3 μmol/kg/d). The drugs were administered via the tail vain for 14 days from the day after the alginate particles were planted, and the mice were free to eat and drink during the experiment. At the end of the administration, parts of the mice were directly sacrificed, the alginate particles were exposed to the back skin, and the surface angiogenesis of the particles was photographed and stained using H&E. The mice were then injected with 1% FITC-dextran (100 mg/kg) via the tail vein and were sacrificed after 20 min. The alginate particles were then removed, soaked in 1 mL of saline, and thoroughly mixed, and the supernatant was centrifuged. The optical density of the fluorescence in the supernatant was measured using a fluorescent microplate reader (Thermos Scientific). At the same time, the standard curve was made using FITC-dextran.

The antitumor activity of AS16 and mPEG-AS16 *in vivo*

The ascites of the mice were removed and centrifuged at 1,000 rpm for 5 min, and the precipitated S180 cells were resuspended in saline. The survival rate of the cells was over 95%, as measured by 0.2% trypan blue staining. The cell density was adjusted to 1×10^7 cells/mL, and 0.1 mL of cell suspension was injected into the right upper extremities of the mice. The tumor-bearing mice were randomly divided into six groups, with six mice in each group. These groups were the NS group, the AS16 group (0.3 μmol/kg/d), the $mPEG_{5k}$-AS16 high-dose group (0.3 μmol/kg/d), the $mPEG_{5k}$-AS16 low-dose group (0.15 μmol/kg/d), the $mPEG_{20k}$-AS16 high-dose group (0.3 μmol/kg/d), and the $mPEG_{20k}$-AS16 low-dose group (0.15 μmol/kg/d). The drugs were administered *via* the tail vein for 14 days from the third day after the tumor had been administered, and the mice were free to eat and drink during the experiment. The long diameter (a) and short diameter (b) of the tumor were measured daily, and the tumor volume was calculated according to the following formula: Tumor volume = $\pi/6 \times a \times b^2$. The growth curve of the tumor was also drawn. The bodies of the mice were weighed daily, and a body weight curve was drawn. At the end of the administration, the mice were sacrificed, and the tumors were removed and weighed. The tumor inhibition rate of each group was calculated according to the following formula: Inhibition Rate (IR) = (1- tumor weight of the drug group/tumor weight of the NS group) × 100%. The tumor was then subjected to CD31 immunohistochemical staining.

Statistical analysis

Statistical analysis was performed using SPSS 19.0. Experimental data were expressed as mean ± SD. Differences in significance were compared using t test, where *P<0.05, **P<0.01, and ***P<0.001.

Results

Modification and purification of AS16 by PEG

Modification yield is related to pH, time, molar ratio, and temperature of the reaction. mPEG-MAL is able to modify mercapto groups at a fixed point in alkaline and neutral to slightly acidic mediums. After trying different pH levels, we found that there was no significant difference in modification rate in the range of pH 6.0~8.0 (data not shown). Moreover, mPEG-MAL is generally unstable in alkaline environments and prone to ring opening reactions [19]. Thus, we set the pH of the reaction to 6.0. The molecular weight of the peptide was small, and the modified group could be fully exposed. When mPEG-MAL reacted with Cys-AS16 for 1 h, the modification rate was already high. Therefore, in order to determine the best reaction conditions, we, for the most part, varied only the molar ratio and the reaction temperature. The peak times of AS16 and $mPEG_{5k}$-MAL were measured to be approximately 13 and 17 min, respectively. After the reaction, a new peak appeared at approximately 18 min, this being the absorption peak of $mPEG_{5k}$-AS16 (Figure 1A). When the molar ratio of $mPEG_{5k}$-AS16 and Cys-AS16 was 1:1, the modification was unimodal (Figure 1B). When the molar ratio of $mPEG_{5k}$-MAL and Cys-AS16 changed from 1:1 to 2:1, the unreacted $mPEG_{5k}$-MAL gradually increased, but the modification rate did not. The modification rate when the modification reaction temperature was 4°C was significantly higher than that when the temperature was 25°C (Figure 1C, 1D). When the reaction temperature was 25°C, there was a miscellaneous peak at 15.2 min, this being likely due to the peptide degrading at 25°C. However, when the molar ratio of AS16 and $mPEG_{20k}$-MAL was 1:1, the peak times of both $mPEG_{20k}$-MAL and $mPEG_{20k}$-AS16 were approximately 20 min (Figure S1A), and the peak height of $mPEG_{20k}$-MAL was very low. After $mPEG_{20k}$-MAL reacted with AS16, the peak height of $mPEG_{20k}$-AS16 increased significantly. Therefore, although the peak times of AS16 and $mPEG_{20k}$-MAL were close, AS16 was modified by $mPEG_{20k}$-MAL, and the modification rate was high. Considering the separation and purification of the product and the cost of the raw material, the best modification conditions were as follows: pH of 6.0, a molar ratio of 1:1, a temperature of 4°C, and a reaction time of 1 h. Given these conditions, the reaction modification rate was able to exceed 80%. We thus reacted mPEG-MAL with AS16 under these optimal modification conditions and purified the modified compounds

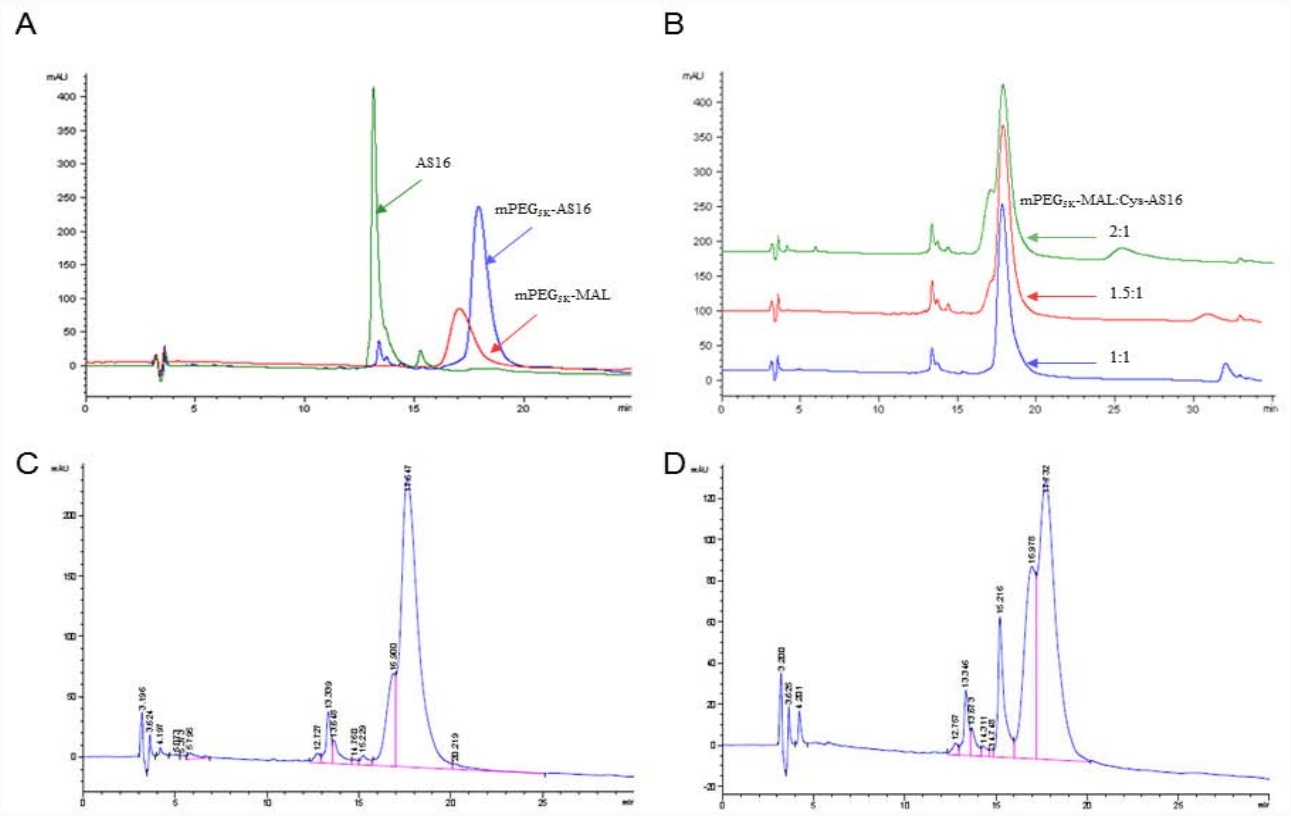

Figure 1: The effect of the molar ratio of Cys-AS16 to $mPEG_{5K}$-MAL and reaction temperature on the modification reaction. A) RP-HPLC chromatogram of modified reactions of AS16 (green line), $mPEG_{5K}$-MAL (red line), and $mPEG_{5K}$-AS16 (blue line). B) Reacting with Cys-AS16 with different molar ratios of $mPEG_{5K}$-MAL. C) A modification reaction RP-HPLC chromatogram at a reaction temperature of 4°C. D) A modification reaction RP-HPLC chromatogram at a reaction temperature of 25°C.

using Reversed-Phase High-Performance Liquid Chromatography (RP-HPLC) [20]. The compounds were separated and purified by preparative RP-HPLC, and $mPEG_{5k}$-AS16 and $mPEG_{20k}$-AS16 were obtained. According to the RP-HPLC analysis of the purified products, $mPEG_{5k}$-AS16 and $mPEG_{20k}$-AS16 had purity of over 90% (Figure S1B, S1C). The modification conditions were mild, and both the reaction rate and modification rate were high. Next, we verified that the PEG modification strategy was able enhance the anti-enzymatic hydrolysis ability of AS16 and extend its half-life *in vivo*.

Study of enzyme stability and preliminary pharmacokinetics of AS16 and its analogues

AS16 had poor stability *in vivo* and had almost completely degraded after 5 h in human plasma (Figure 2A). However, $mPEG_{5k}$-AS16 and $mPEG_{20k}$-AS16 were degraded by about 20% and 10%, respectively, at 200 h because of their significantly reduced enzymatic hydrolysis rate. This reduction was caused by the shielding effect of PEG, the higher molecular weight of the modifier, and the stronger resistance of the drug to enzymatic degradation.

We conducted a preliminary study of the metabolism of AS16 and its modifications *in vivo*. We found that there were no absorption peaks in the blank plasma samples around the maximum absorption peaks of AS16, $mPEG_{5k}$-AS16, and $mPEG_{20k}$-AS16, which suggests that the endogenous substances in the plasma did not interfere with the determination of AS16 and its analogues and that the samples have strong specificity under such chromatographic conditions (Figures S2A-S2C). The AS16, $mPEG_{5k}$-AS16, and $mPEG_{20k}$-AS16 standards were tested using RP-HPLC, the peak area was recorded,

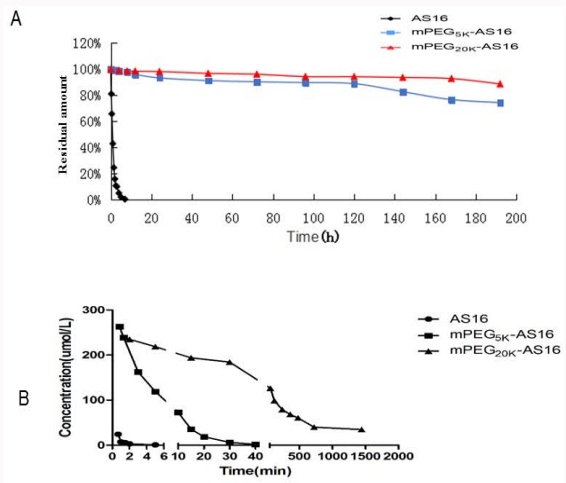

Figure 2: Stability of AS16 and its analogues. A&B) Detect the degradation of AS16, $mPEG_{5K}$-AS16, and $mPEG_{20K}$-AS16 in plasma at 37°C by enzyme hydrolysis stability test.

and linear regression was conducted on the measured peak area (Y) and concentration (X; data not shown). The regression equation of the plasma standard curve of AS16 was Y=1.855X-0.1258 (R2=0.999; a good linear relationship in the range of 3.70 mol/L to 237.68 mol/L). For $mPEG_{5k}$-AS16, the equation was Y=24.069X+2.056 (R2=0.999; a good linear relationship in the range of 7.36 mol/L to 294.72 mol/L). For $mPEG_{20k}$-AS16, the equation was Y=29.152X-1.767 (R^2=0.999; a good linear relation in the range of 23.4 mol/L to 238.68 mol/L).

Table 1: The concentration-time curve of AS16, $mPEG_{5k}$-AS16 and $mPEG_{20k}$-AS16 after i.v. in rats.

Parameters	AS16	$mPEG_{5k}$-AS16	$mPEG_{20k}$-AS16
K (min^{-1})	0.645	0.122	1.334×10^{-3}
$T_{1/2}$ (min)	1.074	5.680	519
Vd (L/kg)	1.305	0.095	0.155
AUC (μmol.min/L)	28.147	2035.352	114500
CL (L/h.kg)	50.520	0.695	0.012

Next, we injected AS16 and mPEG-AS16 into rats to preliminarily study the metabolism of these three substances *in vivo*. We calculated the plasma concentration using the standard curve and drew the drug concentration-time curve. AS16 was rapidly metabolized in rats, its blood concentration after 1min of administration was far lower than that of $mPEG_{5k}$-AS16 and $mPEG_{20k}$-AS16, and it could hardly be detected after 5 min of administration (Figure 2B). PEG modification thus significantly improved the pharmacological properties of the peptides *in vivo*, and the half-life of peptides increased drastically according to the molecular weight of the modifier. The *in vivo* half-life of $mPEG_{5k}$-AS16 increased by approximately five times, and the substance was almost undetectable after 40 min of administration. The *in vivo* half-life of $mPEG_{20k}$-AS16 increased by nearly 500 times, and the blood concentration remained high after 24 h.

According to the concentration-time data, we calculated the main pharmacokinetic parameters of AS16 and its analogues (Table 1). Compared with AS16, the *in vivo* half-lives of $mPEG_{5k}$-AS16 and $mPEG_{20k}$-AS16 were long, their area under the curve was high, and there *in vivo* clearance rate was low. The pharmacokinetic characteristics of $mPEG_{5k}$-AS16 and $mPEG_{20k}$-AS16 were also different from one another. $mPEG_{20k}$-AS16 was clearly metabolized slower *in vivo* and was able to remain at a high blood concentration for a long period of time. This is mainly because the molecular weight of $mPEG_{5k}$-AS16 was small and not enough to reduce the glomerular filtration rate. Only when the molecular weight of PEG modifier was greater than 20 kDa did the glomerular filtration rate decrease, thus extending the peptide's half-life.

Effects of AS16 and its analogues on human umbilical vein endothelial (HUVEC) cell migration

PEG modification not only prolongs the half-life of peptides *in vivo*, but it also reduces their bioactivity [21]. The ideal PEG modification thus causes an increase in half-life *in vivo* that is able to compensate for the decrease in bioactivity. In this study, the half-life of AS16 was prolonged after PEG modification, and a high concentration was maintained for a longer time. Next, we studied the biological activity of AS16 and its analogues. Endothelial cell migration is crucial for tumor angiogenesis, so we examined the effect of AS16 and its analogues on HUVEC cell migration using wound healing assay. We found that the cell wound area in the negative control group was almost completely healed at 24 h (Figure 3A). By contrast, most of the AS16, $mPEG_{5k}$-AS16, and $mPEG_{20k}$-AS16 experimental groups were not healed, and the migration distances

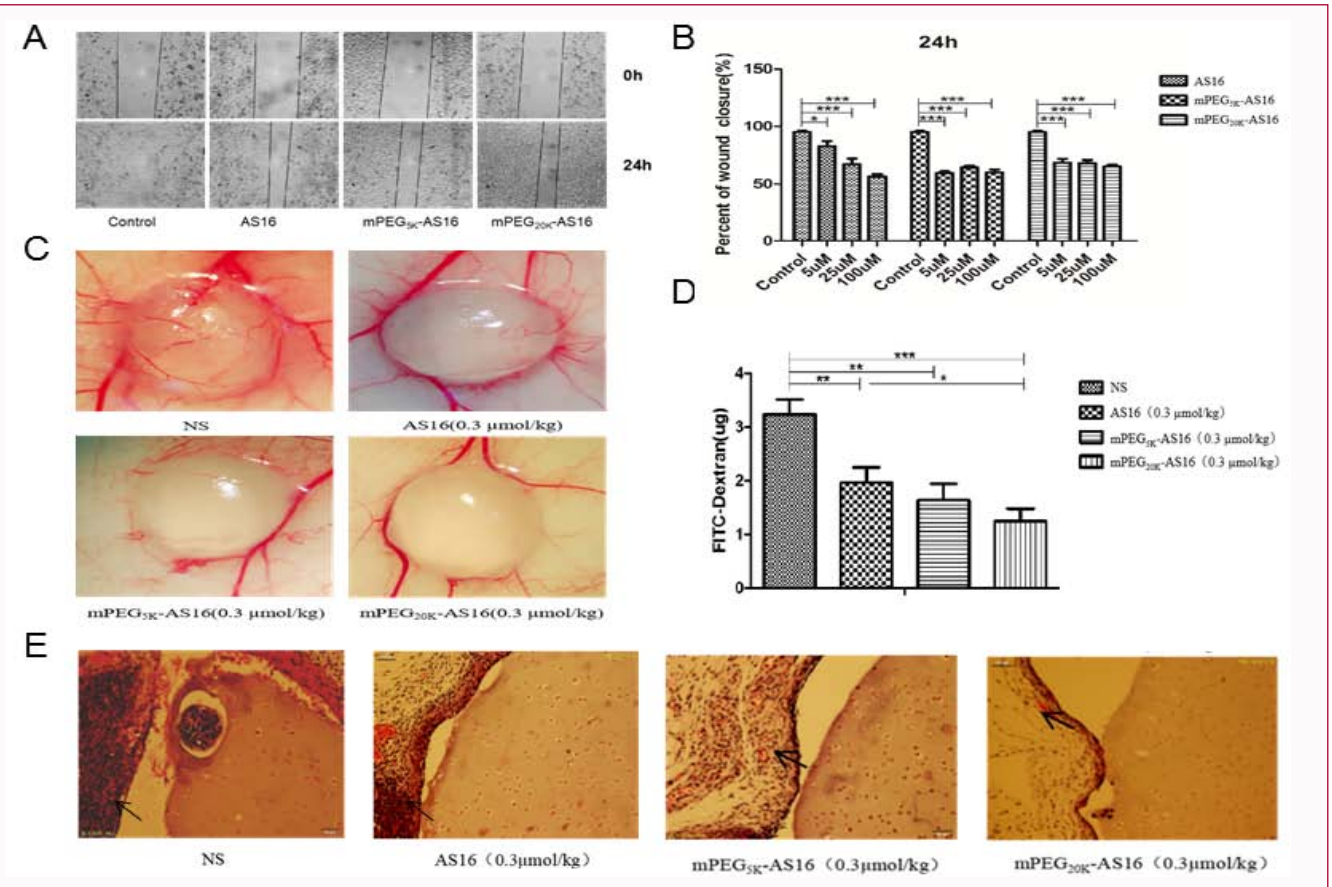

Figure 3: *In vitro* and in vivo biological activities of AS16 and its modifications. A) Representative images of the influence of AS16, $mPEG_{5K}$-AS16, and $mPEG_{20K}$-AS16 on HUVEC cell migration by wound scratch assay. B) Quantification of HUVEC cell mobility. C) Representative images of alginate particles on day 14 after s.c. implantation (4×10^5 cells) into Balb/c mice. D) FITC-Dextran content at alginate particles. Determination of FITC-Dextran was performed after i.v. injection of high molecular weight F1TC-Dextran (100 mg/kg). E) HE staining of alginate particles containing S180 cells. The black arrow points to S180 cells outside the alginate granules. (Magnification: x100). *P<0.05, **P<0.01, ***P<0.001.

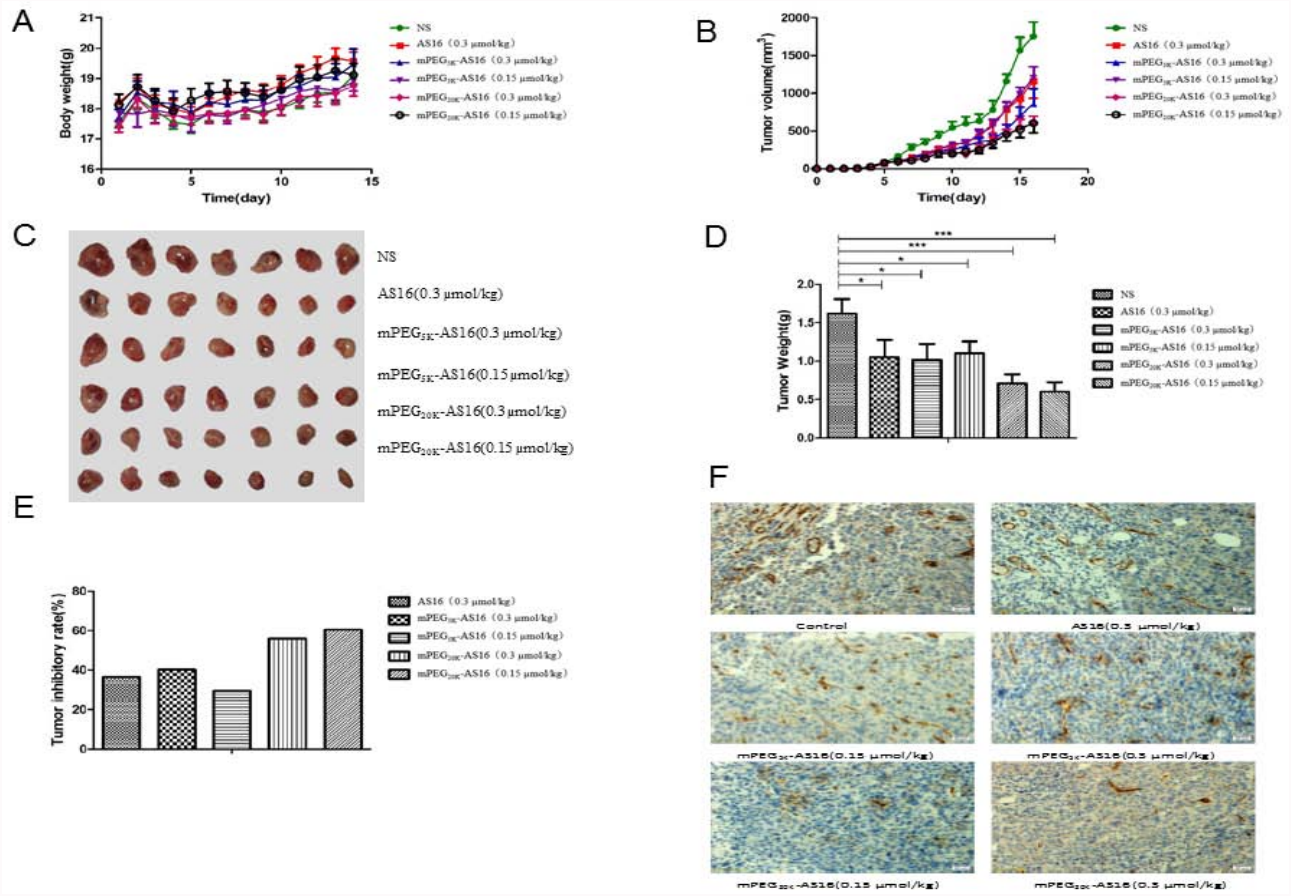

Figure 4: AS16 and its modifications inhibit tumor growth by inhibiting tumor angiogenesis. S180 cells (1.0×10^6 in 100 μl Saline) were injected subcutaneously into the right flanks of Balb/c mice. On the third day after tumor challenge, tumor bearing mice were divided randomly into six groups (n=8). All the mice were killed after 14 days administration with i.v. A) Body weight changes of Balb/c mice. B) The tumor volume-time curves of S180 cells. C) Representative images of tumor tissues. D) Quantification of tumor weights. E) The tumor inhibitory rate of AS16, $mPEG_{5K}$-AS16, and $mPEG_{20K}$-AS16. F) Representative images of CD31 immunostaining on tumor tissues. *P<0.05, **P<0.01, ***P<0.001.

were significantly smaller for these groups than those in the negative control group. According to the results of the wound healing assay, all three peptides were able to significantly inhibit the migration of HUVEC cells (Figure 3B). The ability of AS16 to inhibit HUVEC cell migration was also positively correlated with its concentration. At a concentration of 100 μM, the migration rate was the lowest, about 60%. Both the $mPEG_{5k}$-AS16 and $mPEG_{20k}$-AS16 groups were able to inhibit HUVEC migration, but there was no dose correlation, which may have been because $mPEG_{5k}$-AS16 and $mPEG_{20k}$-AS16 were more stable and able to better perform for a long period of time at a low concentration. $mPEG_{5k}$-AS16 and $mPEG_{20k}$-AS16 had similar effects to that of AS16 in inhibiting HUVEC cell migration, indicating that the biological activity of the original peptide was maintained after PEG modification. This is an important factor in ensuring the effective anti-angiogenesis and antitumor effects of the modifications *in vivo*.

Antitumor angiogenesis in AS16 and its analogues

An alginate-coated S180 cell assay can be used to directly quantify the antitumor angiogenesis of AS16 and its analogues *in vivo*. Thus, we transplanted alginate particles under the skin of mice. Because the tumor cells in the alginate particles released all kinds of factors that promoted angiogenesis, there was angiogenesis on the surface of the particles. The FITC-labeled dextran that binds and adsorbs to the vascular endothelial cells was injected through the tail vein, and then, the fluorescence in the particles was detected to quantitatively determine the vascular density of the alginate particles. We determined that the stronger the fluorescence, the more vessels the alginate particles had. We also observed the alginate particles in each group and found that the vascular densities of the particles in the AS16, $mPEG_{5k}$-AS16, and $mPEG_{20k}$-AS16 groups were significantly reduced (Figure 3C). The anti-angiogenesis ability of $mPEG_{5k}$-AS16 and $mPEG_{20k}$-AS16 was stronger than that of AS16, and there were almost no vessels on the surface of particles in the $mPEG_{20k}$-AS16 group. It was thus found that AS16, $mPEG_{5k}$-AS16, and $mPEG_{20k}$-AS16 were able to effectively inhibit tumor angiogenesis and that $mPEG_{20k}$-AS16 had the strongest anti-angiogenesis effect (Figure 3D). Using Hematoxylin and Eosin (H&E) staining of alginate particles, we found that the tumor cells were mostly dead at the particle centers and that there was a large number of living tumor and vascular endothelial cells on the particle surfaces. The number of surrounding cells of the $mPEG_{20k}$-AS16 group had significantly reduced (Figure 3E), and the cells on the particle surface of the $mPEG_{20k}$-AS16 group had the lowest number, indicating that $mPEG_{20k}$-AS16 was able to inhibit tumor angiogenesis most effectively.

Inhibitory effect of AS16 and its analogues on sarcoma 180 transplant model

Finally, we tested the antitumor activity of AS16 and mPEG-AS16 *in vivo* using Sarcoma 180 (S180) mouse transplant models. During the experiment, the growth status of the mice in each group

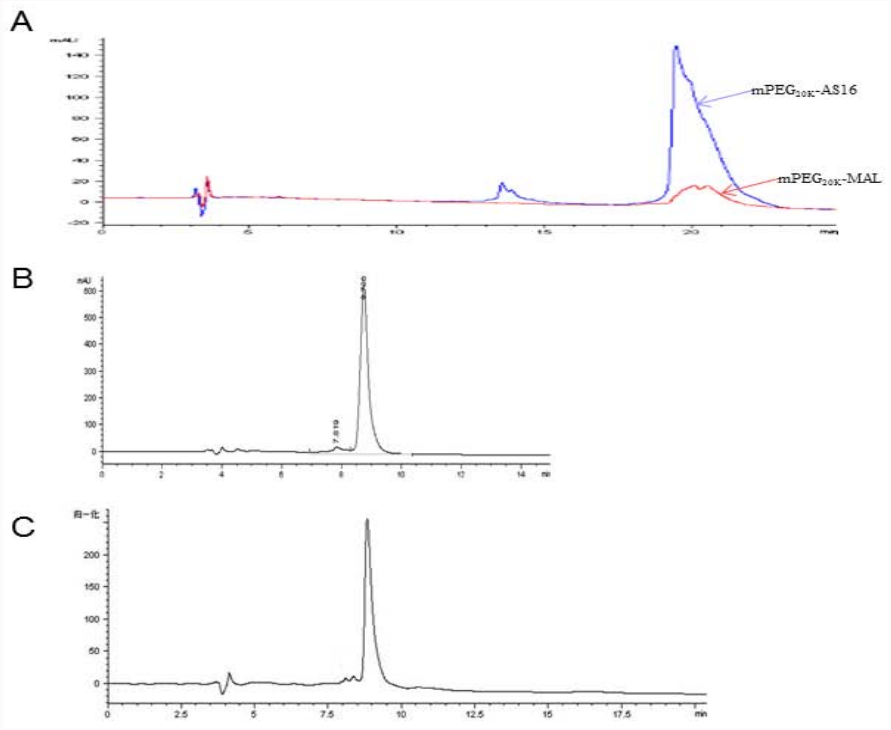

Figure S1: A) RP-HPLC chromatogram of modification reaction of $mPEG_{20K}$-MAL (red line) and $mPEG_{20K}$-AS16 (blue line). B) After the modification reaction is completed, $mPEG_{5K}$-AS16 is separated and purified by preparative RP-HPLC. C) After the modification reaction is completed, $mPEG_{20K}$-AS16 is separated and purified by preparative RP-HPLC.

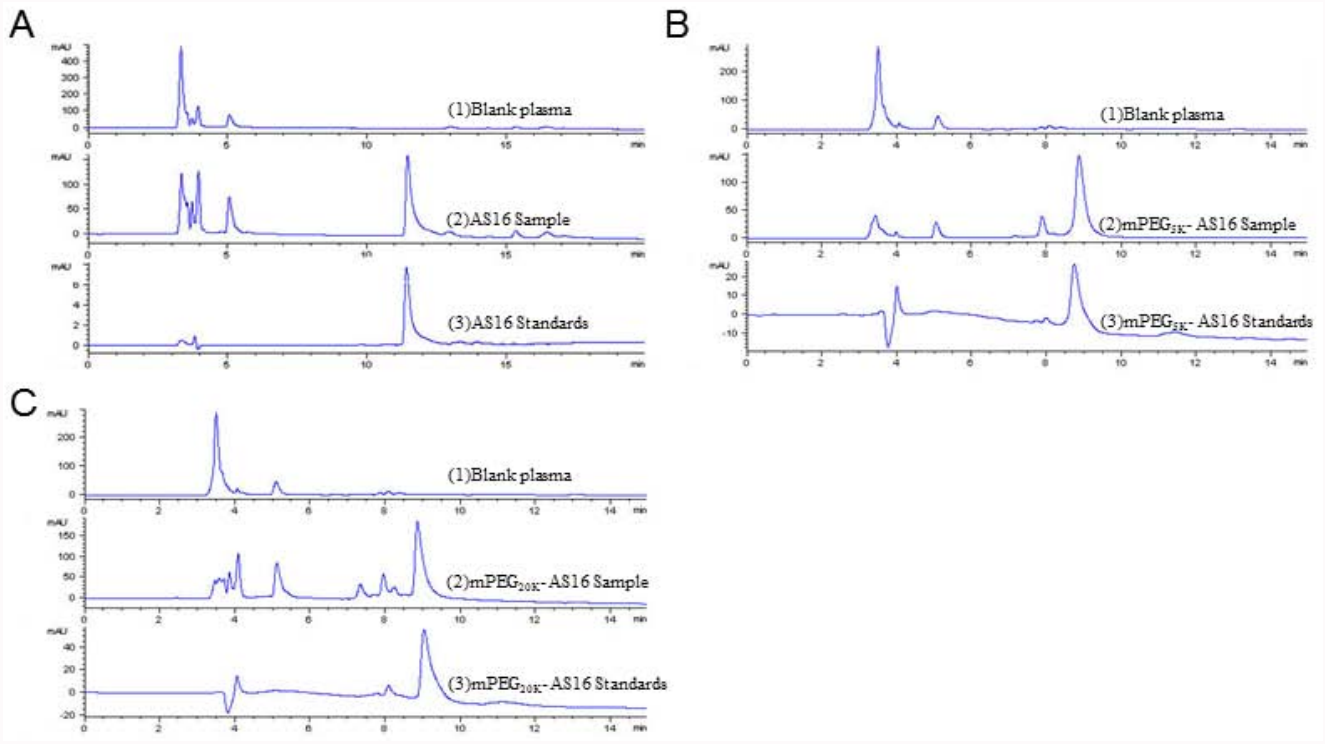

Figure S2: Specificity of the plasma RP-HPLC chromatogram of AS16 and its modifications. A) Plasma RP-HPLC chromatogram of AS16. (1) Blank plasma; (2) plasma sample containing AS16; (3) AS16 standards. B) Plasma RP-HPLC chromatogram of $mPEG_{5K}$-AS16. (1) Blank plasma; (2) plasma sample containing $mPEG_{5K}$-AS16; (3) $mPEG_{5K}$-AS16 standards. C) Plasma RP-HPLC chromatogram of $mPEG_{20K}$-AS16. (1) Blank plasma; (2) plasma sample containing $mPEG_{20K}$-AS16; (3) $mPEG_{20K}$-AS16 standards.

was positive, and the body weight of the mice also increased slowly, indicating that $mPEG_{5k}$-AS16 and $mPEG_{20k}$-AS16 did not have high toxicity because of the extension of *in vivo* half-life (Figure 4A). At the same time, the tumor growth rate slowed significantly in the AS16

group as well as those of its analogues, and the $mPEG_{20k}$-AS16 group had the slowest tumor growth rate (Figure 4B).

Both AS16 and its analogues were able to inhibit tumors, but both the low and high doses of $mPEG_{20k}$-AS16 caused a significantly stronger inhibition of tumor growth compared with the other peptides (Figure 4C, 4D). The tumor inhibition rate of AS16 (0.3 mol/kg) was 36.5%. The tumor inhibition effect of $mPEG_{5k}$-AS16 in the high-dose group (0.3 mol/kg) was slightly better than that in the AS16 group, which had a tumor inhibition rate of 40.2%. The tumor inhibition rate of $mPEG_{5k}$-AS16 in the low-dose group (0.15 mol/kg) was only 29.4% (Figure 4E), slightly lower than that in the AS16 group (0.3 mol/kg). The tumor inhibition rates of the high-dose (0.3 mol/kg) and low-dose (0.15 mol/kg) groups of $mPEG_{20k}$-AS16 were 60.4% and 55.9%, respectively, representing tumor inhibition effects significantly better than those of both AS16 and $mPEG_{5k}$-AS16. In addition to having the best tumor inhibition effect, $mPEG_{20k}$-AS16 retained its biological activity *in vivo*, had a significantly extended half-life, and was able to maintain a high concentration for a long period of time. Thus, our results indicate that even a low dose of $mPEG_{20k}$-AS16 can effectively inhibit the growth of tumors.

Platelet endothelial cell adhesion molecule (CD31) is a marker specifically expressed by vascular endothelial cells. In our study, we used anti-CD31 antibody to perform immunohistochemical staining on tumor tissues to directly observe tumor angiogenesis. Our results revealed that blood vessel density was lower in both the AS16 group and those of its analogues (Figure 4F). The $mPEG_{5k}$-AS16 (0.15 mol/kg) group had a large number of tumor blood vessels, and the $mPEG_{5k}$-AS16 (0.3 mol/kg) group showed no significant difference in blood vessel density to AS16 (0.3 mol/kg). There were, however, significantly fewer blood vessels in the tumor tissues of the $mPEG_{20k}$-AS16 group than in those of the other groups, though there was no significant difference between the high- and low-dose $mPEG_{20k}$-AS16 groups. This was consistent with the tumor inhibition results-the tumor vascular density in the group that had the best tumor inhibition effect was also the lowest.

Discussion

In order to improve the poor stability and short half-life of peptide AS16, we used PEG fixed-point modification technology to modify it, thus obtaining $mPEG_{5k}$-AS16 and $mPEG_{20k}$-AS16 with purity of over 90%. In terms of stability, both $mPEG_{5k}$-AS16 and $mPEG_{20k}$-AS16 demonstrated increased resistance to enzymatic hydrolysis, and the pharmacokinetic parameter results revealed that the half-life of $mPEG_{5k}$-AS16 and $mPEG_{20k}$-AS16 had also been significantly prolonged. *In vivo* functional experiments confirmed that $mPEG_{5k}$-AS16 and $mPEG_{20k}$-AS16 retained their anti-angiogenic activity, and the antitumor effects of $mPEG_{5k}$-AS16 and $mPEG_{20k}$-AS16 were also better than those of AS16 in a mouse transplant model.

The selection of PEG binding sites, the types and sizes of PEG modifiers, and the conditions required for modification are key factors affecting the bioactivity of PEG peptides. It had been reported that the Ala at the N-terminal of AS16 was not an active site [22]. We thus tried using D-Ala to replace the L-Ala at the N-terminal of AS16, and the modified AS16 showed better antitumor activity (data not shown). We made further modifications of the N-terminal of AS16 accordingly. The mercapto groups in peptides and proteins are small, react easily, and are thus ideal modification sites [23]. AS16, however, does not contain sulfhydryl groups. We thus linked a Cysto the N-terminal of AS16 using chemical synthesis to obtain modified precursor Cys-AS16 (CATWLPPRAANLLMAAS) and then modified it at fixed points [24,25]. The fixed-point modification not only led to homogeneous modifications, but it also facilitated the separation and purification of modifications. Because there is a hydroxyl group at both terminals of PEG, the monomethoxy polyethylene glycol with one terminal closed by a methyl group is often used as the modifier in order to prevent cross-linking or clustering during the modification. mPEG-MAL is the most commonly used mercapto fixed-point modifier and is created by adding a sulfide bond to the mercapto group via the double bond in the maleimide ring. The higher the molecular weight of the PEG modifier, the stronger it's shielding effect on the active site of the enzyme on the peptide surface. The molecular weight of the PEG modifier is also positively correlated with the anti-enzymatic hydrolysis ability of the modification as well as its half-life. However, the shielding effect of PEG on the active site of the peptide will also be enhanced, which may significantly reduce the biological activity of the peptide. The selection of them PEG-MAL molecular weight thus requires consideration of the retention of peptide activity and the extension of half-life. In our study, two mPEG-MAL modifiers with molecular weights of 5 ($mPEG_{5k}$-MAL) and 20 kDa ($mPEG_{20k}$-MAL), respectively, were selected to react with free mercapto at the N-terminal of Cys-AS16 to achieve fixed-point modification of the inactive site of AS16.

We also introduced a Cys at the N-terminal of AS16 by chemical synthesis to obtain the modified precursor Cys-AS16. Then, we modified the mercapto group of the N-terminal Cys with $mPEG_{5k}$-MAL and $mPEG_{20k}$-MAL. Functional experiments confirmed that $mPEG_{5k}$-AS16 and $mPEG_{20k}$-AS16 had similar effects to AS16 in inhibiting vascular endothelial cell migration and tumor angiogenesis, indicating that the biological activity of AS16 had been retained. The anti-enzymatic hydrolysis ability of $mPEG_{5k}$-AS16 and $mPEG_{20k}$-AS16 was similar, and the peptide's time curve revealed that the half-life of $mPEG_{20k}$-AS16 was about 91 times that of $mPEG_{5k}$-AS16, indicating that the extension of $mPEG_{20k}$-AS16 half-life is mainly related to the decrease of glomerular filtration rate; this is consistent with the results of a study by Wu et al. [26]. The half-life of $mPEG_{20k}$-AS16 was prolonged, but the bioactivity of $mPEG_{20k}$-AS16 *in vivo* was not changed, though we predicted that it would be increased. Compared with $mPEG_{5k}$-AS16 and AS16, $mPEG_{20k}$-AS16 had better antitumor angiogenesis, which supported our prediction.

In conclusion, chemical modification of AS16 by PEG fixed-point modification technique resulted in a modified product, $mPEG_{20k}$-AS16, with higher stability, longer half-life, and better anti-angiogenesis and antitumor effects than AS16. Compared with NRP1 and Tie2 antibodies or with NRP1 and Tie2 dual-function antibodies, $mPEG_{20k}$-AS16 is a promising peptide antitumor drug with a low price, simple chemical synthesis, and easy preservation.

Acknowledgment

This study was financially supported by the Natural Science Foundation of Henan Province (Grant Nos. 152300410028 and 14A350007).

References

1. Fukumura D, Kloepper J, Amoozgar Z, Duda DG, Jain RK. Enhancing cancer immunotherapy using antiangiogenics: Opportunities and challenges. Nat Rev Clin Oncol. 2018;15(5):325-40.

2. Peterson TE, Kirkpatrick ND, Huang Y, Farrar CT, Marijt KA, Kloepper

J, et al. Dual inhibition of Ang-2 and VEGF receptors normalizes tumor vasculature and prolongs survival in glioblastoma by altering macrophages. Proc Natl AcadSci U S A. 2016;113(16):4470-5.

3. Binetruy-Tournaire R, Demangel C, Malavaud B, Vassy R, Rouyre S, Kraemer M, et al. Identification of a peptide blocking Vascular Endothelial Growth Factor (VEGF)-mediated angiogenesis. EMBO J. 2000;19(7):1525-33.
4. Tournaire R, Simon MP, le Noble F, Eichmann A, England P, Pouysségur J. A short synthetic peptide inhibits signal transduction, migration and angiogenesis mediated by Tie2 receptor. EMBO Rep. 2004;5(3):262-7.
5. Wu D, GaoY, Chen L, Qi Y, Kang Q, Wang H, et al. Anti-tumor effects of a novel chimeric peptide on S180 and H22 xenografts bearing nude mice. Peptides. 2010;31(5):850-64.
6. Bidwell GL. Peptides for cancer therapy: A drug-development opportunity and a drug-delivery challenge. Ther Deliv. 2012;3(5):609-21.
7. Kopecek J. Polymer-drug conjugates: Origins, progress to date and future directions. Adv Drug Deliv Rev. 2013;65(1):49-59.
8. Roberts MJ, Bentley MD, Harris JM. Chemistry for peptide and protein PEGylation. Adv Drug Deliv Rev. 2002;54(4):459-76.
9. Veronese FM, Pasut G. PEGylation, successful approach to drug delivery. Drug Discov Today. 2005;10(21):1451-8.
10. Pasut G, Veronese FM. State of the art in PEGylation: The great versatility achieved after forty years of research. J Control Release. 2012;161(2):461-72.
11. Nischan N, Hackenberger CP. Site-specific PEGylation of proteins: Recent developments. J Org Chem. 2014;79(22):10727-33.
12. Dozier JK, Distefano MD. Site-specific PEGylation of therapeutic proteins. Int J Mol Sci. 2015;16(10):25831-64.
13. Zhang C, Yang XL, Yuan YH, Pu J, Liao F. Site-specific PEGylation of therapeutic proteins via optimization of both accessible reactive amino acid residues and PEG derivatives. Bio Drugs. 2012;26(4):209-15.
14. Chapman AP. PEGylated antibodies and antibody fragments for improved therapy: A review. Adv Drug Deliv Rev. 2002;54(4):531-45.
15. Kolate A, Baradia D, Patil S, Vhora I, Kore G, Misra A. PEG - a versatile conjugating ligand for drugs and drug delivery systems. J Control Release. 2014;192:67-81.
16. Kang JS, Deluca PP, Lee KC. Emerging PEGylated drugs. Expert Opin Emerg Drugs. 2009;14(2):363-80.
17. Becker R, Dembek C, White LA, Garrison LP. The cost offsets and cost-effectiveness associated with PEGylated drugs: A review of the literature. Expert Rev Pharmacoecon Outcomes Res. 2012;12(6):775-93.
18. Alconcel SNS, Baas AS, Maynard HD. FDA-approved poly(ethylene glycol)-protein conjugate drugs. Polymer Chemistry. 2011;2(7):1442-8.
19. Liu J, Wang Z, He J, Wang G, Zhang R, Zhao B. Effect of site-specific PEGylation on the fibrinolytic activity, immunogenicity, and pharmacokinetics of staphylokinase. Acta Biochim Biophys Sin (Shanghai). 2014;46(9):782-91.
20. Park EJ, Lee KC, Na DH. Separation of positional isomers of mono-poly(ethylene glycol)-modified octreotides by reversed-phase high-performance liquid chromatography. J Chromatogr A. 2009;1216(45):7793-7.
21. Pasut G. Pegylation of biological molecules and potential benefits: Pharmacological properties of certolizumab pegol. BioDrugs. 2014;28(Suppl 1):S15-23.
22. Starzec A, Ladam P, Vassy R, Badache S, Bouchemal N, Navaza A, et al. Structure-function analysis of the antiangiogenic ATWLPPR peptide inhibiting VEGF(165) binding to neuropilin-1 and molecular dynamics simulations of the ATWLPPR/neuropilin-1 complex. Peptides. 2007;28(12):2397-402.
23. Kontermann RE. Strategies for extended serum half-life of protein therapeutics. Curr Opin Biotechnol. 2011;22(6):868-76.
24. Gao M, Tian H, Ma C, Gao X, Guo W, Yao W. Expression, purification, and C-terminal site-specific PEGylation of cysteine-mutated glucagon-like peptide-1. Appl Biochem Biotechnol. 2010;162(1):155-65.
25. Pan LQ, Wang HB, Lai J, Xu YC, Zhang C, Chen SQ. Site-specific PEGylation of a mutated-cysteine residue and its effect on Tumor Necrosis Factor (TNF)-Related Apoptosis-Inducing Ligand (TRAIL). Biomaterials. 2013;34(36):9115-23.
26. Ling Wu, Ho SV, Wang W, Gao J, Zhang G, Su Z, et al. N-terminal mono-PEGylation of growth hormone antagonist: Correlation of PEG size and pharmacodynamic behavior. Int J Pharm. 2013;453(2):533-40.